

# On the expected $\gamma$ -ray emission from nearby flaring stars

S. Ohm<sup>1</sup> and C. Hoischen<sup>2</sup>

<sup>1</sup>*The Deutsches Elektronen-Synchrotron (DESY), D-15738 Zeuthen, Germany*

<sup>2</sup>*Institut für Physik und Astronomie, Universität Potsdam, Karl-Liebknecht-Strasse 24/25, D-14476 Potsdam, Germany*

Accepted 2017 October 25. Received 2017 October 16; in original form 2017 September 18

## ABSTRACT

Stellar flares have been extensively studied in soft X-rays (SXR) by basically every X-ray mission. Hard X-ray (HXR) emission from stellar superflares, however, have only been detected from a handful of objects over the past years. One very extreme event was the superflare from the young M-dwarf DG CVn binary star system, which triggered *Swift*/BAT as if it was a  $\gamma$ -ray burst. In this work, we estimate the expected  $\gamma$ -ray emission from DG CVn and the most extreme stellar flares by extrapolating from solar flares based on measured solar energetic particles (SEPs), as well as thermal and non-thermal emission properties. We find that ions are plausibly accelerated in stellar superflares to 100 GeV energies, and possibly up to TeV energies in the associated coronal mass ejections. The corresponding  $\pi^0$ -decay  $\gamma$ -ray emission could be detectable from stellar superflares with ground-based  $\gamma$ -ray telescopes. On the other hand, the detection of  $\gamma$ -ray emission implies particle densities high enough that ions suffer significant losses due to inelastic proton–proton scattering. The next-generation Cherenkov Telescope Array (CTA) should be able to probe superflares from M dwarfs in the solar neighbourhood and constrain the energy in interacting cosmic rays and/or their maximum energy. The detection of  $\gamma$ -ray emission from stellar flares would open a new window for the study of stellar physics, the underlying physical processes in flares and their impact on habitability of planetary systems.

**Key words:** radiation mechanisms: non-thermal – stars: flare – stars: individual: DG CVn – gamma rays: stars.

## 1 INTRODUCTION

Flares are a common phenomenon in the Sun, stars and young stellar objects (see e.g. Benz & Güdel 2010, for a recent review). They typically result from a restructuring of the stellar magnetic field and manifest themselves in a release of magnetic energy by reconnection. In these reconnection events, ionizing radiation is produced and particles are accelerated to non-thermal energies. Flares, especially in young stars, are important as the released radiation and energetic particles can influence outer planetary atmospheres by heating and ionization (e.g. Segura et al. 2010; Venot et al. 2016). The most extreme flares to date are observed in X-rays from nearby M-dwarf stars.

DG CVn is a young (30 Myr) M-dwarf binary star system located at 18 pc distance to the Sun. At least one of its member stars is a rapid rotator. This system underwent an extreme flaring event on 2014 April 23 (Drake et al. 2014), which triggered the Burst Alert Telescope (BAT) aboard the *Swift* satellite, and caused it to slew automatically to the source as if it was a  $\gamma$ -ray burst. The BAT detected DG CVn in the hard X-ray (HXR) band between 15–150 keV

with a peak flux of  $\sim 300$  mCrab. The  $\gamma$ -ray superflare is one of only a handful detected by *Swift* in a decade, and was  $\sim 200$  thousand times more energetic in X-rays than X-class solar flares (class X1 corresponds to  $3 \times 10^{26}$  erg s<sup>-1</sup>). The first flaring episode lasted for 2.2 h, and had a total energy in the 0.3–10 keV energy band of  $4 \times 10^{35}$  erg. The day after, a second flare occurred, which had a similar radiated energy as the first one, and lasted for 6.4 h (Osten et al. 2016). Different episodes of the superflare were observed by the XRT and UVOT instrument onboard *Swift* after the repositioning. Also other ground-based optical instruments followed-up on the BAT alert. The results of these observations are reported in detail elsewhere (Caballero-García et al. 2015; Osten et al. 2016). As part of the AMI-LA Rapid Response Mode (ALARRM), prompt radio follow-up observations were taken at 15 GHz within 6 min of the burst. Fender et al. (2015) reported on the detection of a bright ( $\sim 100$  mJy) radio flare in these observations. An additional bright radio flare, peaking at around 90 mJy, occurred around 1 yr later. In high-energy  $\gamma$  rays ( $100 \text{ MeV} \leq E \leq 100 \text{ GeV}$ ), Loh, Corbel & Dubus (2017) searched for a counterpart in archival *Fermi*-LAT data. The authors found a transient event (but happening in 2012), at a position consistent with DG CVn, which they associate to be a likely flaring background blazar. The imaging atmospheric Cherenkov telescope (IACT) system MAGIC operates in the

\* E-mail: stefan.ohm@desy.de

very-high-energy domain ( $50 \text{ GeV} \leq E \leq 50 \text{ TeV}$ ) and followed up on this flare within 30 s after the alert and observed it for 3.3 h (Mirzoyan 2014). The authors placed an upper limit on the energy flux above 200 GeV of  $1.2 \times 10^{-11} \text{ erg cm}^{-2} \text{ s}^{-1}$ .

Given the characteristics of the superflare from DG CVn and other systems, we argue in this paper that events like the one in 2014 are potentially detectable by current- and next-generation IACTs such as MAGIC, VERITAS, HESS or the future Cherenkov Telescope Array (CTA). In Section 2, we shortly review the properties of solar flares with focus on particle acceleration and high-energy  $\gamma$ -ray emission. Section 3 discusses if and how properties of solar flares can be extrapolated to stellar flares. In Section 4, we present two possible scenarios for particle acceleration in the DG CVn event and apply a non-thermal emission model to estimate the expected  $\gamma$ -ray emission in the tens of GeV energy range and above. In Section 5, we will extend the non-thermal emission model to the population of nearby young dwarf stars and estimate the number of potentially detectable stellar flares with the upcoming CTA.

## 2 SOLAR ENERGETIC PARTICLES AND $\gamma$ -RAY PRODUCTION IN SOLAR FLARES

Most of the knowledge about physical mechanisms at work in stellar flares has been acquired in studies of solar flares. Especially, highly relativistic particles that are released in stellar flares are notoriously difficult to study. Radio cyclotron and gyrosynchrotron emission originate from thermal and mildly relativistic electrons up to MeV energies. Higher energy electrons can in principle be studied via their non-thermal X-ray emission. But the HXR emission detected in stellar flares is better described as the tail of a thermal hot plasma (50–100 MK), rather than a non-thermal thick-target bremsstrahlung component. At  $\gamma$ -ray energies, no stellar flare has been detected to date, and studies of relativistic protons and nuclei and their impact on the surroundings of these stars are limited to extrapolations from solar flares (e.g. Segura et al. 2010).

Solar flares are observed across the electromagnetic spectrum from radio to  $\gamma$  rays. Contrary to stellar flares, non-thermal HXR synchrotron emission from relativistic electrons has been detected from the Sun up to tens of MeV. At  $\gamma$ -ray energies, flare-accelerated ions excite heavier nuclei when impinging on the chromosphere, and subsequently emit nuclear  $\gamma$ -ray lines. Neutrons produced in the spallation of nuclei in large flares are captured by protons, which produce the deuterium recombination line at 2.22 MeV. This recombination line allows one to infer the flux, spectrum and total energy of ions. At even higher energies of 100 MeV and above, continuum radiation is emitted by ions inelastically scattering with ambient nuclei, which produce charged and neutral pions. Neutral pions decay into two  $\gamma$  rays that can be studied with instruments such as the *Fermi*-LAT. Over the past couple of years, the  $\gamma$ -ray emission at hundreds of MeV to GeV energies from solar flares has been studied in quite some detail. The quiescent sun has been studied by Abdo et al. (2011), whereas solar flares have been investigated by Ackermann et al. (2012), Ajello et al. (2014) and Ackermann et al. (2014). Pesce-Rollins et al. (2015) and Ackermann et al. (2017) reported on three behind-the-limb (BTL) solar flares. The findings of these works can be summarized as follows: (i) Particle acceleration is more common in solar flares than previously thought. (ii) The short, impulsive phase of flares can be followed by a longer duration phase that can last up to several hours. (iii)  $\gamma$ -ray emission is associated with flares that are accompanied by fast coronal mass ejections (CMEs). (iv) Accelerated protons better describe the spectral energy distribution than accelerated electrons. (v) Maxi-

mum  $\gamma$ -ray energies of several GeV imply the presence of tens of GeV protons and nuclei in the acceleration region.

Two main scenarios for the acceleration of solar energetic particles (SEPs) are established by now: Impulsive events, triggered by magnetic reconnection, produce steep particle spectra ( $dN/dE \propto E^{-\alpha}$ ,  $\alpha \simeq 3.0$ ) that are highly enriched in  $^3\text{He}$  and heavier ions. Gradual SEP events, on the other hand, are caused by extensive acceleration in coronal and interplanetary shock waves (typically associated to fast and energetic CMEs), which produce harder particle spectra that extend to higher energies (e.g. Reames 2013). Extreme events can sometimes produce GeV protons that shower in Earth's atmosphere and lead to a detectable increase in neutron flux at ground level (so called ground level enhancements, GLEs).

The spectral and temporal characteristics of solar flares that have been observed with *Fermi* so far can be interpreted in both scenarios: Some flares show  $\gamma$ -ray emission coincident with the HXR impulsive emission (Ackermann et al. 2012). The majority of flares, however, shows longer emission indicative of continuous acceleration in a stochastic turbulence process in the solar corona and interaction in the solar upper atmosphere (Ackermann et al. 2014). Alternatively, continuous acceleration takes place in the shocks of the CME, and  $\gamma$  rays are produced when particles are travelling along field lines back to the photosphere and interact there (Ackermann et al. 2017).

One limitation of the LAT and other spacecrafts designed to detect  $\gamma$  rays and energetic particles from the sun is their detection area, which is too small to detect the highest energy photons, electrons or ions even in solar flares. Ground-based IACTs, on the other hand, have sufficient detection area, are operating in the tens of GeV to TeV energy range, but cannot observe the sun directly. Extensive air shower arrays like HAWC or the planned LHAASO detector will be able to search for solar  $\gamma$ -ray emission in the TeV energy range (Zhou et al. 2017).

## 3 PARTICLE ACCELERATION AND $\gamma$ -RAY PRODUCTION IN STELLAR FLARES

### 3.1 Energetics requirements

Next, we will explore if the  $\gamma$ -ray emission from stellar flares can potentially be detected from nearby active stars with *Fermi*-LAT or IACTs. The fact that no stellar flare from any nearby star has ever been observed above X-ray energies requires us to combine the knowledge about solar flares that have been studied in particles and  $\gamma$  rays up to a few GeV, with stellar flares that are typically seen in radio and optical wavelengths and up to X-ray energies. The energetics estimates and scaling from the Sun to stellar flares rely on three main assumptions, which will be discussed in detail as follows:

- (i) The underlying physical processes in solar and stellar flares are similar. This will allow us to infer the energy in accelerated particles in stellar flares in nearby stars.
- (ii) The energy in accelerated electrons is similar to the energy in accelerated protons.
- (iii) In stellar superflares, equipartition holds between radiated (thermal) X-ray energy and energy in accelerated electrons. This allows us to use the measured X-ray flux to infer the energy in accelerated protons, independent of the thermal/non-thermal origin of X-rays.

### 3.1.1 Stellar flares resemble solar flares

As outlined in Osten et al. (2016), the interpretation of the DG CVn stellar superflare event assumes that the same physical processes are at work as in the solar case. In general, this assumption is supported by many stellar observations, and scaling relations from solar to stellar flares have been inferred from observations at extreme UV or soft X-rays (SXR; Aschwanden, Stern & Güdel 2008). Multiwavelength observations show that the inferred properties of the plasma and non-thermal particles in stellar flares resemble that of solar flares. For instance, the time evolution of the plasma temperature and density is similar in solar and stellar flares (see e.g. Benz & Güdel 2010, and references therein). The most striking correlation in this regard is probably the linear relation between radio gyro-synchrotron emission and thermal X-rays, which spans more than 6 orders of magnitude in X-ray and radio luminosity from solar microflares to the most extreme stellar flares observed in EQ Peg (cf. fig. 11 in Benz & Güdel 2010).

### 3.1.2 Energy in electrons and protons is comparable

As described in detail in Benz & Güdel (2010), ions accelerated in solar flares impinge on the chromosphere and excite heavy ions. In the subsequent de-excitation process, nuclear lines are emitted and can be used to infer the ion spectrum, flux and total energy. Of special importance is the neutron capture line at 2.223 MeV. In solar flares, Ramaty et al. (1995), for instance, find that the energy in protons with energies above 1 MeV is comparable to the energy stored in non-thermal electrons above 20 keV. This result is confirmed by, for example, Emslie et al. (2005). More recently, also Emslie et al. (2012) studied the relation between energy released in electrons and ions in solar flares. The authors found that, for the sample of strong solar flares that were accompanied by SEPs and CMEs, the energy content in flare accelerated electrons and ions was comparable. However, the estimates in these works are afflicted with a considerable uncertainty and are only valid as order of magnitude estimates mainly due to the uncertain low-energy cut-off in the electron spectrum and the extrapolation of the ion spectrum to higher energies. Moreover, not all strong flares are followed by CMEs and/or SEPs.

### 3.1.3 Equipartition holds between thermal and non-thermal X-rays

Isola et al. (2007) find a remarkable correlation between SXR and HXR radiation from solar flares to the most extreme stellar flares. The correlation between SXRs (which trace the thermal plasma) and radio emission (which trace non-thermal electrons) suggests that one can employ the X-ray emission in stellar flares as a tracer for the energy content in relativistic electrons and ions, independent of a thermal/non-thermal origin of the X-rays. Indeed, Emslie et al. (2012) studied the global energetics of large solar flares and found that the total SXR radiation from the hot plasma is comparable to the energy stored in high-energy electrons with energies greater than 20 keV.

## 4 NON-THERMAL EMISSION MODEL

To produce  $\gamma$ -ray emission at a level detectable by IACTs, two more conditions have to be fulfilled: acceleration of particles to very high energies with hard  $\gamma$ -ray spectra and high enough densities for the

production of  $\pi^0$ -decay  $\gamma$  rays. The maximum energy and spectral index of the relativistic proton population in the DG CVn flare is probably the most critical and least constrained property in the model presented below. In analogy to solar flares, we will nevertheless try to estimate both quantities in two scenarios: particle acceleration and  $\gamma$ -ray production in the impulsive phase as a result of magnetic reconnection and gradual particle acceleration via diffusive shock acceleration in the CME that very likely accompanied the flaring event.

The DG CVn superflare is characterized in optical, radio and X-rays by two episodes (see Caballero-García et al. 2015; Fender et al. 2015; Osten et al. 2016). The first impulsive episode lasted for approximately 400 s and was denoted ‘big first flare’ (BFF). The BFF was followed by a second flaring episode (called F2) that started around  $8 \times 10^3$  s and peaking at  $10^4$  s after the BFF peak. The second flaring episode lasted for about 6.4 h in X-rays (Osten et al. 2016) and 4–5 d in radio (Fender et al. 2015). The total duration of this exceptional event was more than 2 weeks in X-rays.

### 4.1 Particle acceleration and $\gamma$ -ray production in the BFF

The arguments made in Section 3.1 suggest that we can use the measured X-ray emission from stellar flares as a proxy for the energy content in relativistic protons and nuclei accelerated in the prompt phase of the DG CVn event. Maximum particle energies associated with prompt solar flares and as measured by *Fermi* reach a few GeV ( $\leq 400$  MeV in  $\gamma$  rays) within 1 min (Ackermann et al. 2012). Although particle acceleration in impulsive solar flares is established, the underlying physical mechanism is not well understood. Various models exist that link the magnetic reconnection event more directly or indirectly to the particle acceleration process (see e.g. Knizhnik, Swisdak & Drake 2011, and references therein). For the sake of argument and to guide the reader, we follow the argumentation of Takahashi, Mizuno & Shibata (2016), who derive a maximum proton energy as  $E_{\max} \sim 7 \text{ GeV } B_{100} V_{100} L_{0.1 R_s}$ . Here,  $B_{100}$  is the active region’s (AR’s) magnetic field strength in 100 G,  $V_{100}$  is the ‘inflow’ plasma speed in  $100 \text{ km s}^{-1}$  and  $L_{0.1 R_s}$  is the length-scale of the AR in 0.1 solar radii. If equipartition holds in the DG CVn superflare, the magnetic fields inferred by Osten et al. (2016) are between a few hundred Gauss and several kG in the coronal loops, and several kG on the stellar surface. These magnetic field estimates are consistent with independently inferred magnetic fields, based on equipartition between gas pressure and magnetic pressure. Such large magnetic fields would, in principle, allow for a fast acceleration of particles similar to solar flares, but to higher maximum energies than observed for the Sun (Osten et al. 2016). Assuming their best-fitting estimate of  $B_{\text{BFF}} = 580$  G at the site of magnetic reconnection and an AR length-scale of  $0.1 R_s$  (i.e.  $0.25 R_*$ ), the maximum proton energy would be around 40 GeV. Only for somewhat extreme magnetic fields of several kG and AR sizes comparable to the stellar disc of DG CVn, one would reach maximum energies approaching 1 TeV. Even if these extreme conditions could be met, proton spectra in solar flares have typically indices of  $\alpha = 3.0$  or steeper. The best-fitting spectral proton index in a hadronic scenario for the impulsive flare studied by Ackermann et al. (2012) even has an index of  $\alpha \geq 4.5$ . Nevertheless, we will explore how the  $\gamma$ -ray spectral energy distribution would look like and how they compare to the sensitivity of the *Fermi*-LAT and the next-generation CTA.

As discussed in Section 2, observations of solar flares with *Fermi* show that the high-energy  $\gamma$ -ray emission can last for hours,

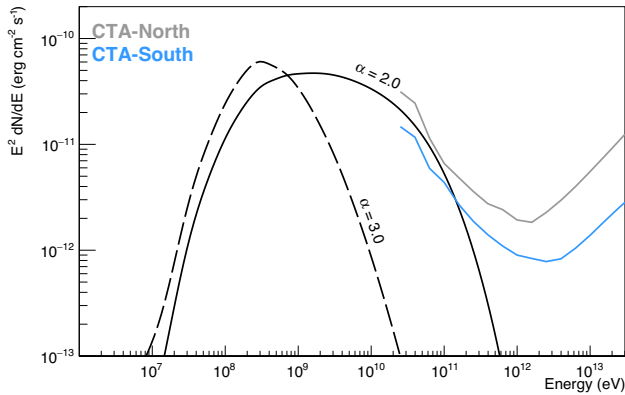


**Figure 1.** Expected  $\gamma$ -ray emission from the BFF based on the time-dependent injection and interaction model for protons as described in the main text. Solid curves depict the  $\pi^0$ -decay  $\gamma$ -ray emission from protons with cut-off energy  $E_c = 1$  GeV and index  $\alpha = 2.0$ . Dashed curves show the emission for protons with  $E_c = 100$  GeV and  $\alpha = 3.0$ . Also shown are the CTA-South and CTA-North integral sensitivities for the duration of the flare of 2 h for the BFF. The 1-day *Fermi*-LAT upper limit from Loh et al. (2017) would be around  $2.7 \times 10^{-9}$  erg cm $^{-2}$  s $^{-1}$ , assuming a mean photon energy of 3 GeV.

although the short impulsive phase typically seen at X-ray energies only lasts for seconds to minutes (see e.g. Ackermann et al. 2014, and references therein). Given the characteristics of impulsive solar flares, we explore two cases here, which could be seen as realistic and optimistic. Injection of protons according to a power law in energy with an exponential cut-off of the form

$$dN(E)/dE = N_0 E^{-\alpha} \exp(-E/E_c),$$

within 2 h in the BFF with a minimum energy of  $E_{p,\min} = 1$  GeV and (1) with a cut-off energy of  $E_c = 50$  GeV and  $\alpha = 3.0$ , and (2) with a cut-off energy of  $E_c = 500$  GeV and  $\alpha = 2.0$ . In both cases, the energy in injected protons corresponds to the total energy in electrons as inferred by Osten et al. (2016) based on the *Swift* data between 0.3 and 10 keV. As described above, we assume energy partition between electrons and protons, and hence adopt the electron number density in the coronal loop as inferred by Osten et al. (2016) of  $N_e = 3 \times 10^{11}$  cm $^{-3}$  as target density for  $pp$  interactions. In all considerations, we adopt a distance to DGCvN of 18 pc. Fig. 1 shows the resulting  $\pi^0$ -decay  $\gamma$ -ray spectra of the two BFF scenarios in a time-dependent model for the injection and interaction of relativistic protons based on the radiative code by Hinton & Aharonian (2007). Also shown is the expected CTA sensitivity.<sup>1</sup> Interestingly, in a high-density environment such as the one considered here, the cooling time of protons is comparable to their injection time, i.e.  $\tau_{pp} \simeq 1.6$  h. This implies that, independent of maximum energy and energy content in accelerated particles, a significant fraction of the energy injected in protons is radiated at  $\gamma$ -ray energies and not released into interplanetary space as stellar energetic particles.

It is clear that only in the optimistic scenario,  $\gamma$ -ray emission at a level detectable by CTA is produced. Reducing the minimum energy for the injected protons from 1 GeV to 100 MeV would reduce the

<sup>1</sup>Integral energy flux sensitivities have been obtained using the public CTA performance files (<https://www.cta-observatory.org/science/cta-performance/>), ignoring systematic errors and assuming a background normalization value of  $\alpha = 0.05$ .

level of  $\gamma$ -ray emission in the extreme scenario by  $\sim 25$  per cent. Note that the 1-day LAT upper limit by Loh et al. (2017) is about an order of magnitude higher than the predicted emission level at any energy.

## 4.2 Particle acceleration and $\gamma$ -ray production in the F2

Energetic particles released in solar flares are often accelerated to hundreds of MeV and GeV energies. IACTs, however, have an energy threshold in the tens of GeV energy range, requiring particle acceleration to hundreds of GeV up to TeV energies in stellar flares. The highest energy particles and GLE events are often associated with massive and fast CMEs (e.g. Gopalswamy et al. 2012). Although faster CMEs tend to produce higher energy particles more efficiently, there is a large scatter of SEP intensities released in these gradual events, independent of CME properties. There is increasing evidence that the most energetic SEP and GLE events are associated with a population of supra-thermal particles pre-accelerated in preceding large flares (e.g. Reames 2000; Kahler 2001), often from the same AR (Gopalswamy et al. 2004). Generally, quasi-parallel shocks are able to accelerate more protons and nuclei out of the thermal pool of solar/stellar wind particles, but not to sufficiently high energies and typically with steep spectra. Quasi-perpendicular shocks, on the other hand, are able to accelerate particles to higher energies faster and produce harder particle spectra. However, injection into the shock region is hampered as it is harder for particles to catch up with the shock and enter the acceleration process (Kozarev & Schwadron 2016). A supra-thermal seed particle population allows for both, an efficient injection into quasi-perpendicular shocks and a fast acceleration to high energies (e.g. Ng & Reames 2008; Laming et al. 2013). In fact, the extreme solar flare from 2005 January 20 is a good example to support this hypothesis: This event was preceded by several X-class solar flares from the same AR and the resulting final SEP spectrum had a hard particle index of  $\alpha = 2.14$  (Mewaldt et al. 2012).

### 4.2.1 Energy in relativistic protons in CME shock

The strongest solar flares are associated almost 1:1 with fast and equally energetic CMEs (Emslie et al. 2012). The direct imaging of stellar CMEs is implausible with current instruments, due to which indirect measures are needed to detect stellar CMEs and to infer their properties, such as speed or mass loss (e.g. Leitzinger et al. 2011; Kay, Opher & Kornbleuth 2016, and references therein). In the following, we will assume that the F2 event in DGCvN is accompanied by a CME. Using the findings of Emslie et al. (2012) again, the kinetic energy in a CME is approximately an order of magnitude larger than the energy in non-thermal electrons and ions. The energy in SEPs, on the other hand, is about 5 per cent of the CME kinetic energy. For the sake of argument and given the large uncertainties, we will in the following assume that the energy in SEP is the same as the energy in flare-accelerated electrons, i.e.  $9 \times 10^{35}$  erg for F2. We base our estimates of the dynamics of the CME in F2, i.e. the mass lost during the event and the speed of the ejecta, on the empirical relation between flare energy and mass-loss in T Tauri star superflares and solar flares as discussed by Aarnio, Matt & Stassun (2012, cf. their fig. 1). For a kinetic energy of  $E_{\text{CME,kin}} = 9 \times 10^{36}$  erg, equation (2) of Aarnio et al. (2012) gives an ejected mass in the range of  $m_{\text{CME}} = (4.9 \times 10^{19} - 3.8 \times 10^{21})$  g. Guided by the case for solar flares (e.g. Mewaldt et al. 2012), we will adopt here a CME velocity of  $v_{\text{CME}} = 3000$  km s $^{-1}$ , which

gives an ejected mass of  $m_{\text{CME}} = 1.8 \times 10^{20}$  g – in agreement with Aarnio et al. (2012).

#### 4.2.2 Maximum energy of accelerated particles

Estimating the maximum particle energy that can be achieved in the CME shock acceleration process is challenging, but can again be based on solar flares and associated CME acceleration. Simulations of particle acceleration in parallel shocks show that particle energies of hundreds of MeV energies can be achieved within 10 min in a CME of  $2500 \text{ km s}^{-1}$  (Ng & Reames 2008). Kozarev & Schwadron (2016), on the other hand, developed a data-driven analytical model, and find that with slower shock speeds of  $800 \text{ km s}^{-1}$  and acceleration in quasi-perpendicular shocks, maximum energies of several GeV can be reached in the same time. Scaling these results to the duration of the DG CVn flare of 10 h, and ignoring non-linear effects such as proton-amplified Alfvén wave growth, suggests that maximum particle energies of 20 GeV in the case of a fast and quasi-parallel shock, and 100 GeV in case of a quasi-perpendicular shock, can be reached. In the Kozarev & Schwadron (2016) model, a constant magnetic field of 5 G was assumed. In reality, acceleration in the CME shock will proceed under changing conditions, and the magnetic field will drop as the CME expands as  $R^{-2}$  (Kay et al. 2016). An assumed 20 kG field – typical for an M-dwarf AR magnetic field – would have dropped to  $\sim 20$  G after 2 h, and to about  $\sim 1$  G after 10 h for the assumed shock speed of  $v_{\text{CME}} = 3000 \text{ km s}^{-1}$ . Since the detailed modelling of particle acceleration under changing magnetic field conditions is beyond the scope of this paper, we will assume that acceleration proceeds in a constant magnetic field of 10 G. If indeed strong shocks are present in the CME, maximum particle energies of 200 GeV for fast parallel shocks and 1 TeV for somewhat slower quasi-perpendicular shocks are possible. The real conditions under which particle acceleration in the CME proceeds is much more complex, as, for example, the shock morphology will change from quasi-perpendicular to quasi-parallel as the CME expands. As discussed above, if the origin of the two DG CVn flares was indeed the same AR, the coronal and ejected particles from the BFF will have very likely been pre-accelerated. This would result in a more efficient injection into the F2 CME shock and acceleration to higher particle energies and with hard spectra. To summarize, particle acceleration in the fast and dense CME that was likely associated to the DG CVn F2 event to energies beyond 100 GeV and possibly up to TeV energies seems plausible.

The maximum energy particles can be accelerated to is limited either by the acceleration time (i.e. the duration of the flare) or by the  $pp$  loss time. The acceleration time  $\tau_{\text{acc}}$  in a strong shock and in the Bohm limit (i.e. the theoretically fastest possible acceleration) is

$$\tau_{\text{acc}} \approx 1.4 \text{ h } v_{\text{CME}, 10^3 \text{ km s}^{-1}}^{-2} E_{100 \text{ GeV}} B_{\text{G}}^{-1}.$$

The  $pp$  loss time is (e.g. Hinton & Hofmann 2009)

$$\tau_{pp} \approx 2.6 \text{ h } n_{11}^{-1},$$

with  $n$  being the target density in  $10^{11} \text{ cm}^{-3}$ . Especially at early times, the  $pp$  cooling time is short, as the density in the CME is very high. As the density drops as  $\rho_{\text{CME}} \propto t^{-3}$  and the magnetic field only falls like  $B \propto t^{-2}$ , the maximum energy of particles will increase over the duration of the flare. Once the  $pp$  cooling time becomes shorter than the duration of the flare, the maximum particle energy will drop linearly over time again. For an initial magnetic field in the AR of  $B_0 = 5 \text{ kG}$ , and a CME shock speed of

$v_{\text{CME}} = 3000 \text{ km s}^{-1}$ , maximum particle energies will increase from 100 GeV after 15 min to about 6 TeV after 5 h, and drop to 1.5 TeV after 10 h. These estimates should not be taken at face value: They rely on the assumption of a strong shock and  $pp$  interaction in a homogeneous medium. If acceleration operates in weaker shocks, lower maximum energies are to be expected. On the other hand, if only a fraction of protons interact downstream of the shock, the bulk can be accelerated to higher energies earlier on.

#### 4.2.3 Expected $\gamma$ -ray emission from the F2 event

In the following, we will explore different scenarios to give a rough overview over the expected  $\gamma$ -ray emission under varying (but constant) conditions. We will close this chapter by exploring a time-dependent scenario that could be seen as representative for the conditions in the F2 flare in this model.

As discussed in Section 4.2.1, it is assumed that material with a mass of  $m_{\text{CME}} = 1.8 \times 10^{20}$  g is ejected in the CME and moving with a speed of  $v_{\text{CME}} = 3000 \text{ km s}^{-1}$ . With this assumed CME velocity and mass, the density would drop after 5 h to  $n_{\text{CME}} = 1.6 \times 10^{11}$ , and particles would start to leave the system, as the  $pp$  cooling time would be comparable to the flare duration. Protons are injected constantly over the duration of the F2 event and according to a power law in energy with exponential cut-off of the form

$$dN(E)/dE = N_0 E^{-\Gamma} \exp(-E/E_c),$$

with proton spectral index  $\Gamma = 2.0$  and cut-off energy  $E_c = 1 \text{ TeV}$ . In a first attempt to study the expected emission from F2, all parameters are fixed and only the total energy in protons is varied. Fig. 2 shows the expected  $\gamma$ -ray emission for three proton cut-off energies, and for three different injection energies, while leaving the other quantity at a fixed value.

In this simplified model,  $\gamma$ -ray emission from an event similar to the DG CVn flare would be visible for the F2 episode with both CTA-North as well as CTA-South for events where 10 per cent of the potential CME kinetic energy can be transferred to accelerated protons, and if protons are accelerated to energies higher than 1 TeV. If the maximum proton energy reaches 300 GeV, this event would still be visible with CTA-South. For a fixed maximum proton energy of 1 TeV, on the other hand, the F2 event would be visible from both CTA sites if  $\gtrsim 7$  per cent of the CME kinetic energy were transferred to accelerated protons. As discussed in Emslie et al. (2012), about 5 per cent of the CME kinetic energy is transferred to SEPs in solar flares. In this case, the F2 event would be visible with CTA-South, but not CTA-North. In all scenarios, a low energy threshold is key to study the potential  $\gamma$ -ray emission in the high-energy cut-off region.

As discussed in Section 4.2.1 and the beginning of this section, conditions such as the magnetic field, target density and maximum particle energy change as the CME moves outwards. Next, we will try to address this by exploring different environmental conditions, which could be seen as representative for the early, mid and late phases of the F2 event. Table 1 summarizes the assumed input parameters, and Fig. 3 shows the expected  $\gamma$ -ray emission for such a model. The early phase can be characterized by acceleration in a very dense medium with somewhat lower maximum energies. It is followed by a phase, where the  $pp$  cooling time is comparable to the flare duration and particles start to leave the system. Here, the highest maximum energies are expected to be achieved in the presented model. At later times, the maximum particle energy will drop, as the magnetic field decays. As the CME

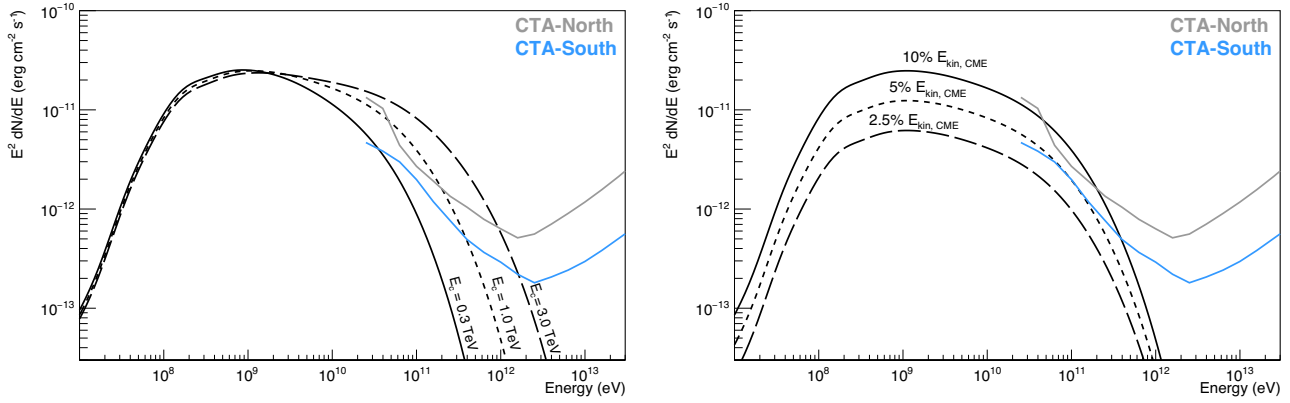


**Figure 2.** Expected  $\gamma$ -ray emission of the F2 in the non-thermal emission model as described in the main text and in Fig. 1. Shown are models with varying proton cut-off energy (left-hand panel,  $E_{inj} = 9 \times 10^{35}$  erg) and fractions of CME kinetic energy that are transferred to high-energy protons (right-hand panel,  $E_c = 1$  TeV). In all models, an average density of  $n_{CME} = 1.6 \times 10^{11}$  and injection over a time of 10 h is assumed. Also shown are the integral energy flux sensitivities for the two proposed CTA sites for an exposure of 10 h.

**Table 1.** Summary of input parameters for the time-dependent injection model for the three representative phases of F2 as discussed in the main text and shown in Fig. 3.

Phase	Duration (h)	$E_{pp}$ ( $10^{35}$ erg)	$E_{max}$ (TeV)	$\rho$ ( $10^{11}$ cm $^{-3}$ )
Early	3.0	2.7	0.3	30
Mid	4.0	3.6	1.0	1.5
Late	3.0	2.7	0.8	0.5

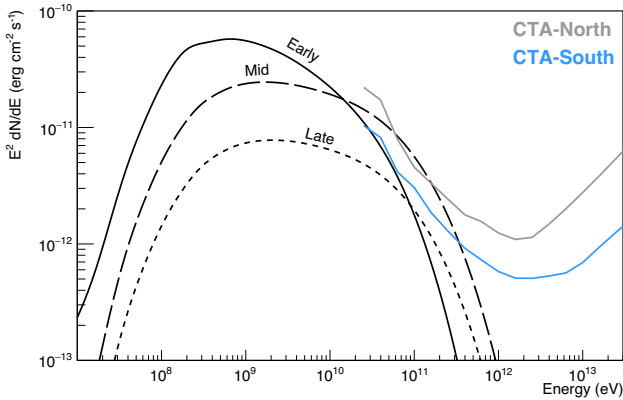


**Figure 3.** Expected  $\gamma$ -ray emission of the three representative F2 in the non-thermal emission model as described in the main text and in Table 1. Also shown are the integral energy flux sensitivities for the two proposed CTA sites for an assumed observation time of 4 h.

material is thinning out over time, densities are falling below a critical value, where no more detectable  $\gamma$ -ray emission is expected and the bulk of accelerated particles is assumed to leave the system as stellar energetic particles. Interestingly, planets situated in the habitable zone around M-dwarf stars are very close to the central star ( $\sim 0.1$  au, Kay et al. 2016). This implies that for such extreme events as the one seen from DG CVn and the shock speeds assumed above, the CME will impact planets situated in the habitable zone while the system is still calorimetric (i.e. all accelerated protons will interact). For the extreme (and more frequent) events, densities should drop below the calorimetric limit before reaching the habitable zone. In reality, the situation is much more complex and a fraction of the accelerated particles will escape ahead of the shock,

whereas others will stay in the acceleration process or interact downstream with the released CME material producing  $\pi^0$ -decay  $\gamma$  rays.

## 5 EXPECTATION FOR THE POPULATION OF NEARBY YOUNG STARS

Stellar superflares are exceptional events and only a handful have been studied in detail so far. Table 2 summarizes the studied superflares and their properties. In the model described above, and based on the properties such as fluence and duration, all superflares would have been within reach of CTA. In a systematic search for flares with the MAXI/GSC instrument aboard the ISS, Tsuboi et al. (2016) found only 13 stars to be flaring out of a population of 256 active binary stars (Eker et al. 2008). Some of these stars flared multiple times and experienced radiative energy releases of up to  $10^{39}$  erg. Given the infrequency of these large and energetic flares that would potentially be visible for Cherenkov telescopes, the occurrence rate is rather hard to predict. Osten et al. (2016) estimated flares with  $U$ -band energy releases similar to the DG CVn event to happen about once every 5 months for YZ CMi and EV Lac, and once every 3 yr for EQ Peg, which immediately reduces the number of flares that are possible to follow up by 10–15 per cent. Although the frequency of these superflares is rather uncertain, about one event per year should be energetic enough such that observations with MAGIC, HESS or VERITAS<sup>2</sup> should be able to constrain the here proposed model, the energy in protons and the maximum proton energy.

## 6 CONCLUSIONS AND OUTLOOK

We have estimated the  $\gamma$ -ray emission from flaring, nearby, young M-dwarf stars using the X-ray properties of the DG CVn superflare and extrapolations from solar flares. In the considered scenario,  $\gamma$ -ray emission from the DG CVn event in the BFF at a level detectable by the future CTA is possible if equipartition holds between non-thermal electrons and ions, and if particles are accelerated to TeV energies with hard particle spectra. Hard particle spectra and acceleration to TeV energies seem to be challenging at least in this impulsive phase of the flare.  $\gamma$ -ray emission in gradual solar flares

<sup>2</sup> Assuming that the sensitivity of current generation instruments is a factor 5–10 worse than CTA-South.

**Table 2.** List of nearby active stars and recorded superflares, their energetics, duration and fluence.

Object	Distance (pc)	Flare energy ( $10^{34}$ erg)	Fluence ( $10^{-5}$ erg $\text{cm}^{-2}$ )	Energy range	Duration (h)	Reference
AD Leo	4.9	1.0	0.35	(1800 – 8000) Å	4.0	Hawley & Pettersen (1991)
II Peg	42.0	600	2.9	(0.01 – 200) keV	>3.3	Osten et al. (2007)
EV Lac	5.0	5.8	1.9	(0.3 – 10) keV	1.7	Osten et al. (2010, 2016)
DG CVn	18.0	(40 + 90) <sup>a</sup>	3.4	(0.3 – 10) keV	>8	Osten et al. (2016)
EQ Peg	6.5	9.0	1.8	(2.0 – 20) keV	1.1	Tsuboi et al. (2016)
AT Mic	10.2	30	2.4	(2.0 – 20) keV	1.7	Tsuboi et al. (2016)
YZ CMi	5.9	<20	<4.8	(2.0 – 20) keV	<1.5	Tsuboi et al. (2016)

Note. <sup>a</sup>Energy released in BFF and F2.

and associated SEPs have been detected up to several GeV, implying acceleration of particles to tens of GeV energies in the CMEs. We argued that particle acceleration in the F2 event of the DG CVn flare could be realized and that acceleration to high energies with hard particle indices is plausible. Considering the extreme conditions in young M-dwarf stars such as their fast rotation periods, strong magnetic fields and energetic eruptions compared to the Sun, it is not unrealistic to assume that particles are accelerated to hundreds of GeV energies in M-dwarf flares. If detected, the discovery of  $\gamma$ -ray emission from a single star would represent a major breakthrough in stellar physics and mark the detection of GeV  $\gamma$  rays from the first stellar object other than the Sun. It would also give insights into particle acceleration and interaction in stellar atmospheres. Furthermore, it would give a handle on the cosmic ray flux near young stars that are often considered to host exoplanets but experience much stronger flares than observed in the Sun. Studies suggest that cosmic-rays accelerated in stellar flares can have a significant astrobiological effect on exoplanetary atmospheres. A flare from the star system AD Leo for instance (which was 20 times fainter than the DG CVn flare) is estimated to have removed the ozone layer of a potential exoplanet over the course of 2 yr, with a recovery time of several decades (Segura et al. 2010). Given the occurrence rate of these strong flares, there is a possibility of a permanent erosion of the ozone layer in exoplanets (Osten et al. 2016).

Large field-of-view optical survey instruments such as the Zwicky Transient Factory (ZTF) or the Large Synoptic Survey Telescope (LSST) will detect an increasing number of strong stellar flares and add to our understanding of the physics of stellar flares and their impact on the habitability of planets. At very high energies, CTA could potentially open a new window for the study of non-thermal particles in stellar flares.

### ACKNOWLEDGEMENTS

We thank the anonymous referee for her/his comments, which considerably improved the quality of the paper. We would also like to thank M. Ackermann, R. Bühler, J.A. Hinton, G. Maier, Ł. Stawarz and A. Taylor for fruitful discussions and careful reading of the manuscript, as well as K. Strotjohann for contributions to an early version of the draft. This paper has gone through internal review by the CTA Consortium.

### REFERENCES

Aarnio A. N., Matt S. P., Stassun K. G., 2012, *ApJ*, 760, 9  
 Abdo A. A. et al., 2011, *ApJ*, 734, 116  
 Ackermann M. et al., 2012, *ApJ*, 745, 144  
 Ackermann M. et al., 2014, *ApJ*, 787, 15  
 Ackermann M. et al., 2017, *ApJ*, 835, 219

Ajello M. et al., 2014, *ApJ*, 789, 20  
 Aschwanden M. J., Stern R. A., Güdel M., 2008, *ApJ*, 672, 659  
 Benz A. O., Güdel M., 2010, *ARA&A*, 48, 241  
 Caballero-García M. D. et al., 2015, *MNRAS*, 452, 4195  
 Drake S., Osten R., Page K. L., Kennea J. A., Oates S. R., Krimm H., Gehrels N., 2014, *The Astron. Telegram*, 6121  
 Eker Z. et al., 2008, *MNRAS*, 389, 1722  
 Emslie A. G., Dennis B. R., Holman G. D., Hudson H. S., 2005, *J. Geophys. Res.*, 110, A11103  
 Emslie A. G. et al., 2012, *ApJ*, 759, 71  
 Fender R. P., Anderson G. E., Osten R., Staley T., Rumsey C., Grainge K., Saunders R. D. E., 2015, *MNRAS*, 446, L66  
 Gopalswamy N., Yashiro S., Krucker S., Stenborg G., Howard R. A., 2004, *J. Geophys. Res.*, 109, A12105  
 Gopalswamy N., Xie H., Yashiro S., Akiyama S., Mäkelä P., Usoskin I. G., 2012, *Space Sci. Rev.*, 171, 23  
 Hawley S. L., Pettersen B. R., 1991, *ApJ*, 378, 725  
 Hinton J. A., Aharonian F. A., 2007, *ApJ*, 657, 302  
 Hinton J. A., Hofmann W., 2009, *ARA&A*, 47, 523  
 Isola C., Favata F., Micela G., Hudson H. S., 2007, *A&A*, 472, 261  
 Kahler S. W., 2001, *J. Geophys. Res.*, 106, 20947  
 Kay C., Opher M., Kornbleuth M., 2016, *ApJ*, 826, 195  
 Knizhnik K., Swisdak M., Drake J. F., 2011, *ApJ*, 743, L35  
 Kozarev K. A., Schwadron N. A., 2016, *ApJ*, 831, 120  
 Laming J. M., Moses J. D., Ko Y.-K., Ng C. K., Rakowski C. E., Tylka A. J., 2013, *ApJ*, 770, 73  
 Leitzinger M., Odert P., Ribas I., Hanslmeier A., Lammer H., Khodachenko M. L., Zaqarashvili T. V., Rucker H. O., 2011, *A&A*, 536, A62  
 Loh A., Corbel S., Dubus G., 2017, *MNRAS*, 467, 4462  
 Mewaldt R. A. et al., 2012, *Space Sci. Rev.*, 171, 97  
 Mirzoyan R., 2014, *GRB Coordinates Network*, 16238  
 Ng C. K., Reames D. V., 2008, *ApJ*, 686, L123  
 Osten R. A., Drake S., Tueller J., Cummings J., Perri M., Moretti A., Covino S., 2007, *ApJ*, 654, 1052  
 Osten R. A. et al., 2010, *ApJ*, 721, 785  
 Osten R. A. et al., 2016, *ApJ*, 832, 174  
 Pesce-Rollins M., Omodei N., Petrosian V., Liu W., Rubio da Costa F., Allafort A., Chen Q., 2015, *ApJ*, 805, L15  
 Ramaty R., Mandzhavidze N., Kozlovsky B., Murphy R. J., 1995, *ApJ*, 455, L193  
 Reames D. V., 2000, *AIP Conf. Ser. Vol. 516, Proc. 26th Int. Cosmic Ray Conf.*, Invited, Rapporteur and Highlight Papers, p. 289  
 Reames D. V., 2013, *Space Sci. Rev.*, 175, 53  
 Segura A., Walkowicz L. M., Meadows V., Kasting J., Hawley S., 2010, *Astrobiology*, 10, 751  
 Takahashi T., Mizuno Y., Shibata K., 2016, *ApJ*, 833, L8  
 Tsuboi Y. et al., 2016, *PASJ*, 68, 90  
 Venot O., Rocchetto M., Carl S., Roshni Hashim A., Decin L., 2016, *ApJ*, 830, 77  
 Zhou B., Ng K. C. Y., Beacom J. F., Peter A. H. G., 2017, *Phys. Rev. D*, 96, 023015

This paper has been typeset from a  $\text{\TeX}/\text{\LaTeX}$  file prepared by the author.